Materials Letters 75 (2012) 126–129

Contents lists available at SciVerse ScienceDirect

Materials Letters

journal homepage: www.elsevier.com/locate/matlet

Preparation of mesoporous In_2O_3 nanorods via a hydrothermal-annealing method and their gas sensing properties

Jingjing Zhao [a], Mingbo Zheng [b], Xiaoyong Lai [c], Hongling Lu [a], Nianwu Li [a], Zongxin Ling [a], Jieming Cao [a,*]

[a] Nanomaterials Research Institute, College of Materials Science and Technology, Nanjing University of Aeronautics and Astronautics, Nanjing, Jiangsu Province, 210016, China
[b] National Laboratory of Microstructures, School of Electronic Science and Engineering, Nanjing University, Nanjing, Jiangsu Province, 210093, China
[c] Key Laboratory of Energy Resources and Chemical Engineering, Ningxia University, Yinchuan, 750021, China

ARTICLE INFO

Article history:
Received 19 August 2011
Accepted 19 January 2012
Available online 3 February 2012

Keywords:
In_2O_3 nanorods
Hydrothermal
Mesoporous structure
Nanoparticles
Sensors

ABSTRACT

In this work, we report the simple solid-state formation of mesoporous In_2O_3 nanorods with a quasi-single-crystalline framework. The synthesis is based on controlled thermal oxidative decomposition and re-crystallization of precursor $In(OH)_3$ nanorods obtained from a hydrothermal method without using any surfactants or organic templates. Importantly, the rod-like morphology can be completely preserved after thermal treatment. Due to the intrinsic crystal contraction, a highly mesoporous structure with high specific surface area (up to 103.1 m^2/g) has been created. The textual properties can be tailored by varying the annealing temperature. The gas sensing test results show that mesoporous In_2O_3 nanorods possess satisfactory response to dilute ethanol vapor.

1. Introduction

In_2O_3 is a good n-type semiconductor material with a direct band gap of 3.55–3.75 eV. It can be used in nonlinear optical studies [1], nanoelectronics [2], gas transducers [3–5] and sensors [6]. In_2O_3 used in sensor is expected to have large specific surface area to produce more active surface and right pore size distribution to allow diffusion of active species. In recent years, mesoporous In_2O_3 has attracted great interests because of its high specific surface area and special pore structure. The conventional soft template [7,8] and hard template [9–11] routes were complex and sometimes difficult to handle. In recent years, solvothermal-annealing methods become attractive routes for the synthesis of mesoporous In_2O_3 [12–14], which firstly synthesize indium-based precursor nanostructure via hydrothermal or solvothermal methods and then converted them to mesoporous In_2O_3 via solid-state transformation by further annealing treatment. This method was more convenient than previous template methods. However, expensive surfactants or templates are indispensable to most of these syntheses.

In this paper, we have successfully synthesized rod-like $In(OH)_3$ nanostructures via hydrothermal route without using any surfactants or templates. Mesoporous In_2O_3 nanorods with large Brunauer–Emmett–Teller (BET) surface area were obtained through annealing the as prepared $In(OH)_3$. The gas sensing test results show that mesoporous In_2O_3 nanorods possess satisfactory response to dilute ethanol vapor.

2. Experiment

2.1. Synthesis

All chemicals were analytical grade reagent. In a typical procedure, 0.362 g of $InCl_3 \cdot 4H_2O$ and 0.720 g of urea were dissolved in 50 mL of distilled water, respectively. After vigorous magnetic stirring at room temperature for 10 min, $InCl_3$ solution was slowly dropped into urea solution and stirred for 15 min. Then the mixture was transferred into a 150 mL Teflon-lined stainless steel autoclave, and heated at 130 °C for 12 h. After the reaction finished, autoclave was cooled to the room temperature. The white precipitates were collected by centrifugation and washed with distilled water and ethanol for several times, then dried at 80 °C for 24 h in air. Then, the precursors were annealed in air at 350 °C or 400 °C for 3 h, respectively. The obtained yellowish solid products were nominated as "In_2O_3-350" and "In_2O_3-400", respectively.

2.2. Characterization

The phase purity and crystallinity of the as-prepared samples were characterized by X-ray diffraction (XRD) (Bruker D8 advance). The morphology of particle sizes and crystal structure of the samples were analyzed by transmission electron microscopy (TEM) (JEOL JEM-2100) and scanning electron microscopy (SEM) (LEO 1530). The nitrogen adsorption–desorption analysis was measured with a Micromeritics ASAP 2010 instrument. Gas sensing measurements

* Corresponding author at: College of Materials Science and Technology, Nanjing University of Aeronautics and Astronautics, Nanjing, Jiangsu Province, 210016, China. Tel./fax: +86 25 84895289.
E-mail address: jmcao@nuaa.edu.cn (J. Cao).

0167-577X/$ – see front matter © 2012 Published by Elsevier B.V.
doi:10.1016/j.matlet.2012.01.075

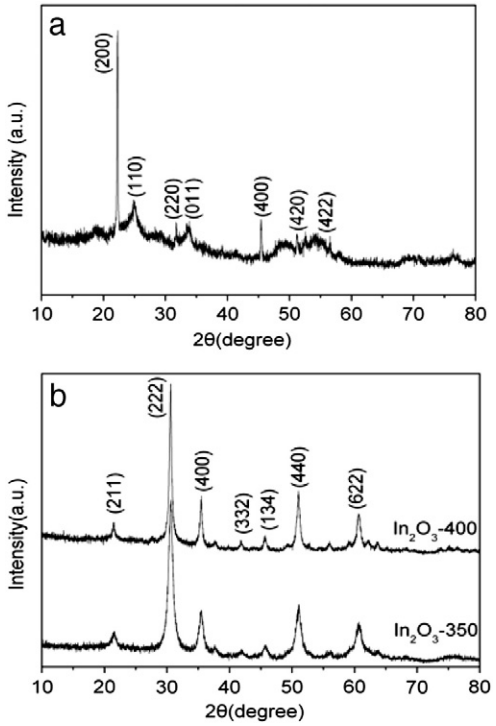

Fig. 1. XRD patterns of $In(OH)_3$ precursor (a) and In_2O_3 (b).

were performed with a computer-controlled WS-30A system (Weisheng Instruments Co., Zhengzhou, China).

3. Results and discussion

Fig. 1(a) shows the XRD pattern of the product of hydrothermal reaction. The five peaks at 22.3°, 31.7°, 45.4°, 51.2° and 56.5° can be indexed to (200), (220), (400), (420) and (422) planes of $In(OH)_3$ (JCPDS 16-0161); meanwhile, the two peaks at 25.9° and 33.7° can be indexed to (110) and (011) planes (JCPDS 17-0549) of InOOH, indicating the existence of a few InOOH. The XRD patterns of In_2O_3 obtained at different annealing temperatures are depicted in Fig. 1(b). The peaks at 21.4°, 30.5°, 35.4°, 41.7°, 45.6°, 50.9° and 60.5° correspond to the (211), (222), (400), (332), (134), (440) and (622) planes of the cubic In_2O_3 (JCPDS 65-3170). No peaks of any other phases or impurities are detected, suggesting the pure phase of the In_2O_3. After annealing treatment, cubic In_2O_3 was obtained by dehydration of $In(OH)_3$. Meanwhile, the small amount of InOOH also transformed into cubic In_2O_3 [15].

The SEM images of precursor $In(OH)_3$ are shown in Fig. 2a–c, which indicates the $In(OH)_3$ sample has the morphology of uniform cylindrical nanorods with rough surface. The diameter of $In(OH)_3$ nanorods is about 600 nm, and the length of them is about 5 μm. The SEM images of In_2O_3-350 (Fig. 2d–f) and In_2O_3-400 (Fig. 2j) reveal that In_2O_3 inherit the cylindrical nanorods morphology after the heat treatment. The TEM images of In_2O_3-350 (Fig. 2g) and In_2O_3-400 (Fig. 2k) display the disordered mesoporous structure of nanorods. Fig. 2h and l show the selected area electron diffraction (SAED) patterns for a single In_2O_3 nanorod of In_2O_3-350 and In_2O_3-400, respectively, which reveal the nanorods possess quasi-single crystal structure. The high-resolution transmission electron microscopy (HRTEM) image of In_2O_3-350 (Fig. 2i) shows clearly crystal lattice stripes, and the planar space of lattice fringes is about 0.293 nm, corresponding to the (222) plane of cubic phase In_2O_3.

The N_2 adsorption–desorption isotherms of In_2O_3 at different annealing temperatures are depicted in Fig. 3. Both the curves can be classified as type IV isotherm. The distinct hysteresis loops can be observed at a relative pressure range from 0.3 to 0.8. The BJH pore size distribution plots of In_2O_3 (inset of Fig. 3) show the existence of pore distributions below 4 nm. In addition, the pore size distribution less than 2 nm cannot be displayed due to the test limitation of the analysis instrument.

The BET surface area of In_2O_3-350 and In_2O_3-400 are 103.1 and 99.7 m^2/g, and the pore volumes are 0.08 and 0.06 cm^3/g, respectively. It is worth noticing that the surface areas of our samples are larger than that (62.6 m^2/g) of the porous single-crystal-like In_2O_3 obtained using InOOH as the precursor [12].

In the hydrothermal process, the formation of $In(OH)_3$ is very closely related to the reaction between In^{3+} and OH^-, which can be described as follows:

$$(NH_2)_2CO + 3H_2O \rightarrow 2NH_4^+ + 2OH^- + CO_2 \quad (1)$$

$$In^{3+} + 3OH^- \rightarrow In(OH)_3 \quad (2)$$

And the high hydrothermal reaction temperature causes small amounts of $In(OH)_3$ to dehydrate as follows:

$$In(OH)_3 \rightarrow InOOH + H_2O \quad (3)$$

When the precursor was heat-treated in air, the following reactions took place:

$$2In(OH)_3 \rightarrow In_2O_3 + 3H_2O \quad (4)$$

$$2InOOH \rightarrow In_2O_3 + H_2O \quad (5)$$

In this procedure, a large amount of H_2O molecules released from the precursor, and molecule-sized pores formed. The molecule-sized pores continually grow into mesoporous structure. Meanwhile, the initially formed In_2O_3 structure units constantly aggregate and grow into In_2O_3 nanoparticles. As a result, nanoparticles and mesopores coexist within the nanorod. The In_2O_3 products have relatively high specific surface area because the mesoporous structure provides plenty of inner surfaces.

Fig. 4 shows the response curves of mesoporous In_2O_3 nanorod sensors to 10–100 ppm ethanol vapors under the operating temperature of 250 °C. When In_2O_3 nanorod sensors are exposed to 100 ppm ethanol vapors, the sensitivity can achieve 12.5. When the temperature decreases to 100 °C, the sensitivity of the sensors can achieve 75, as shown in Table 1. We also detected the sensitivity of these sensors to 100 ppm ethanol vapors at different temperatures in Table 1. The sensitivity increased as the temperature decreased, and it is observed that the gas sensor based on In_2O_3 nanorods exhibits good sensitivity at low temperature but poor stability and the detailed reason still needs be further investigated.

4. Conclusions

In summary, we have demonstrated an effective and green hydrothermal-annealing method to prepare mesoporous In_2O_3 cylindrical nanorods with large BET surface area. The gas sensing tests show that the sensitivity of the mesoporous In_2O_3 can achieve 75 at 100 °C. It is suggested that the mesoporous In_2O_3 is a promising sensor material and is probably to be used practically.

Acknowledgements

This work was financially supported by Natural Science Foundation of Jiangsu Province of China (No. BK2010497), China Postdoctoral Science Foundation (No. 20100471296) and Postdoctoral Foundation of Jiangsu Province (No. 1001003C).